

## Further Insight into the Origin of Potential Oscillations during the Iodate Reduction in Alkaline Solution with Mass Transfer

Z. L. Li,<sup>\*,†,‡</sup> B. Ren,<sup>§</sup> X. M. Xiao,<sup>‡</sup> Y. Zeng,<sup>‡</sup> X. Chu,<sup>‡</sup> and Z. Q. Tian<sup>\*,§</sup>

*Institute of Physical Chemistry and Department of Chemistry, Zhejiang Normal University, Jinhua, Zhejiang 321004 China, State Key Laboratory for Physical Chemistry of Solid Surfaces and Department of Chemistry, Xiamen University, Xiamen 361005 China, and Department of Chemistry, Hunan Normal University, Changsha 410081 China*

*Received: November 12, 2001; In Final Form: March 19, 2002*

In situ Raman spectroscopic studies, in combination with electrochemical measurements, further testify that the electrochemical reactions, i.e., iodate reduction and periodic hydrogen evolution, coupled with alternately predominant diffusion and convection mass transfer of iodate, account for the potential oscillation that appears under galvanostatic reduction of iodate over its limiting current in alkaline solution. The diffusion-limited depletion and the convection-enhanced replenishment of the iodate consist of a pair of positive and negative feedback steps between the bistable states (iodate reduction with and without hydrogen evolution). This mechanism is applicable to the same category of oscillators originating from such a coupling. The limiting diffusion concentration profile and the concentration variation of iodate in the diffusion layer during the oscillation by diffusion-limited depletion and by convection-enhanced replenishment through hydrogen evolution have been measured directly by using in situ Raman spectroscopy for the first time. A crossing cycle in the cyclic voltammogram that displays the bistability and the positive and negative feedbacks can be obtained only when the scan is reversed at a potential where hydrogen evolution takes place, and hydrogen evolution is thus mainly to induce the convection feedback of the reactant after its surface concentration depletes to zero by diffusion-limited reduction, rather than purely an additional current carrier. No oscillation can occur by simply removing the convection feedback with another pure current carrier instead of hydrogen evolution. The other model on the basis of negative differential resistance (NDR) fails to reflect the convection feedback step required for this category of oscillators.

### Introduction

Potential oscillations during electrolysis of alkaline solution of iodate plus highly concentrated iodide ( $2.1 \text{ mol dm}^{-3}$ ) were reported by Radkov and Ljutov.<sup>1</sup> Although the authors observed periodic hydrogen evolution during the oscillations, they did not give any explanation how the oscillations were connected with the hydrogen evolution and only listed some possible chemical and electrochemical reactions. They attributed the oscillations to the coupling reactions between anode and cathode, because they placed the two electrodes very close (2.5 mm) in a test tube of 15 mm inner diameter. We reinvestigated the potential oscillations on different electrodes such as Pt, Ag, and Au,<sup>2</sup> without adding iodide and with the cathode and anode ca. 6 cm apart in a conventional H-type glass cell,<sup>2,3</sup> which exclude the possibility of coupling reactions between anode and cathode during the oscillation as described in ref 1. Potential oscillations still appear above the limiting current, and the oscillatory amplitudes are in the plateau range. No apparent differences were found for the oscillations by using a one-compartment cell or a three-separate-compartment cell, indicating that the oscillation is exclusively from the cathodic process. We proposed that two different electrochemical reactions,  $\text{IO}_3^- + 3\text{H}_2\text{O} + 6\text{e}^- \rightarrow \text{I}^- + 6\text{OH}^-$ <sup>1-2</sup> and  $2\text{H}_2\text{O} + 2\text{e}^- \rightarrow \text{H}_2 + 2\text{OH}^-$  (at the lower potential side of the plateau only), coupled with alterna-

tively predominant diffusion and convection mass transfer account for the potential oscillation (denoted as mechanism A).<sup>2</sup> The key role of hydrogen evolution is to restore the surface concentration of the reactant after its depletion to zero by diffusion-limited reduction. Mechanism A is also applicable to the oscillators for the reduction of ferricyanide,<sup>3</sup> peroxydisulfate,<sup>4</sup> and hydrogen peroxide<sup>5</sup> in alkaline solutions accompanying periodic hydrogen evolution. An alternative theoretical explanation is on the basis of negative differential resistance (NDR),<sup>6</sup> in which iodate reduction current with N-shaped potential dependence due to a Frumkin repulsive effect and an additional current carrier from the hydrogen evolution is emphasized without considering the convection mass transfer (denoted as mechanism B). Extension of mechanism B has also been made to other systems,<sup>6</sup> e.g., the reduction of  $\text{Fe}(\text{CN})_6^{3-}$ .

In this paper, in situ spatiotemporal-resolved Raman spectroscopy and electrochemical measurements were applied to the mechanistic study for the potential oscillations during the reduction of iodate accompanying periodic hydrogen evolution. Our study aims at giving a further insight into the oscillatory origin.

### Experimental Section

Raman spectra were obtained with a LabRam I confocal Raman spectrometer (Dilor, France).<sup>7</sup> The exciting wavelength was 632.8 nm from an air-cooled He–Ne laser with a power of ca. 12 mW. To avoid the interference of the bubbling effect

<sup>†</sup> Zhejiang Normal University.

<sup>‡</sup> Hunan Normal University.

<sup>§</sup> Xiamen University.

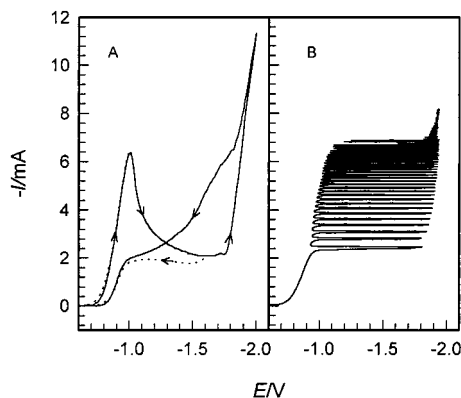


**Figure 1.** Voltammograms by (A) cyclic voltammetry at  $100 \text{ mV s}^{-1}$  with different lower potential limits of  $-2 \text{ V}$  (solid line) and  $-1.6 \text{ V}$  (dotted line), and (B) current scan at  $0.05 \text{ mA s}^{-1}$  in a solution containing  $0.2 \text{ mol dm}^{-3} \text{ IO}_3^-$  and  $1 \text{ mol dm}^{-3} \text{ NaOH}$ .

during the hydrogen evolution, the working electrode surface faced vertically and the spectroelectrochemical cell was mounted on a special optical adapter to enable the irradiation of the laser and the collection of the Raman signal horizontally. A holographic notch filter reflected the exciting line into an Olympus BX40 microscope equipped with a  $\times 50$  long working-length objective (8 mm) so that the objective will not be immersed in the electrolyte. An air-cooled,  $1024 \times 256$  pixels CCD operating in the MPP mode at  $-60^\circ \text{C}$  was used as the detector. The size of the pinhole and slit of the spectrometer were set to 800 and  $200 \mu\text{m}$ , respectively. To obtain the resolution needed for present study, an  $1800 \text{ grooves mm}^{-1}$  grating was used to provide the spectral resolution at  $2\text{--}3 \text{ cm}^{-1}$ . The collection time for recording a single spectrum was 2 s, and the distance of laser focal plane to the electrode surface can be adjusted with micrometric resolution. A detailed description of the spectroelectrochemical cell for Raman microscopy can be found elsewhere.<sup>8</sup> A gold disk (2 mm diameter), a platinum wire in circle, and a saturated calomel electrode (SCE) with a Luggin capillary were employed as the working, counter, and reference electrode, respectively. Electrochemical experiments were carried out with a CHI 660A Electrochemical Station. All solutions were freshly prepared with triply distilled water and analytical grade chemicals.

## Results and Discussion

**Electrochemical Behavior.** There are two ascending branches in the N-shaped curve of the cyclic voltammograms (the solid line in Figure 1A) during the forward scan, which correspond to two different reaction processes (bistable states), i.e., with and without hydrogen evolution; between them there are two overlapping descending branches, which correspond to the diffusion-limited depletion (forward scan) and the convection-induced replenishment (reverse scan) of the iodate concentration near the surface, respectively. The occurrence of a crossing cycle, i.e., the reverse scan current is larger than the forward scan current, can be only explained by the enhanced convection mass transfer of iodate caused by hydrogen evolution in the second up-going branch, because no crossing cycles appear if the potential scan is reversed at a lower potential limit of  $-1.6 \text{ V}$  before hydrogen evolution (the dotted line in Figure 1A). The hydrogen evolution is thus not simply a current carrier<sup>6</sup> but most importantly a source provider of iodate surface concentration through the convection effect, otherwise only an ordinary cyclic voltammogram (no crossing cycles) can be obtained. The numerical result of mechanism B apparently

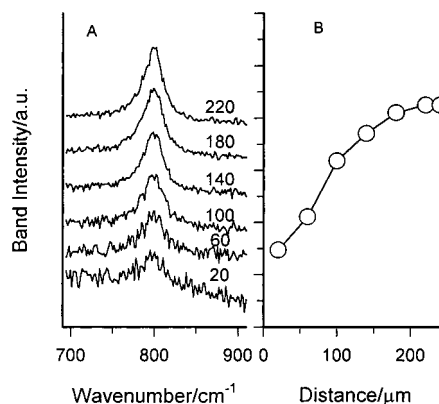


**Figure 2.** (A) In situ Raman spectra at different distance ( $\mu\text{m}$ ) from the electrode surface under a potential control of  $-1.3 \text{ V}$  with a same solution as used in Figure 1, and (B) the relationship of the band intensity with the distance.

contradicts these major experimental facts, noticing that there is a crossing cycle for  $\text{IO}_3^-$  reduction only (the dotted-dashed line in Figure 6a of ref 6).

It may be worth mentioning that a crossing cycle in the cyclic voltammogram means that a pair of overlapping positive and negative feedback steps between the bistable states has found to be a universal topology for oscillatory electrochemical systems, and it is helpful with finding and realizing electrochemical oscillations.<sup>9</sup>

The potential oscillation (Figure 1B) by current scan occurs only above the limiting current accompanying periodic hydrogen evolution at the lower potential side of the limiting current plateau, which also means that the depletion (positive feedback) and replenishment (negative feedback) of the iodate concentration near the surface play the key role in the oscillations.<sup>2</sup>

While in the mechanism B,<sup>6</sup> a negative regulation of rate constant  $k$  with potential  $E$  (with an N or a  $\Lambda$  shape) for the  $\text{IO}_3^-$  reduction is supposed to produce NDR. As  $E$  enters the negative regulation, the reduction rate of the  $\text{IO}_3^-$  drops, then the reduction of  $\text{H}_2\text{O}$  balances the current difference between the applied current  $I$  and the  $\text{IO}_3^-$  current, and the  $\text{IO}_3^-$  surface concentration has the opportunity to recover. Such an explanation also contradicts the fact that the  $\text{IO}_3^-$  reduction is diffusion-controlled, because the descending branch in the N-shaped curve during the forward scan in Figure 1A results from the depletion of the reactant surface concentration due to a faster potential scan ( $100 \text{ mV/s}$ ). By decreasing the scan rate near a steady state ( $2 \text{ mV/s}$ ), a limiting current plateau appears instead (the solid line in Fig. 1 of ref 6) independent of the potential, and hydrogen evolution occurs in the second ascending branch. So the arbitrary choice of a potential-dependent N-shaped rate function for the  $\text{IO}_3^-$  reduction only (eq 8 of ref 6) is inappropriate, and the dashed line in Figure 4 of ref 6 does not reflect the physical reality under the steady state.

**In Situ Raman Spectroscopy.** To our knowledge it is the first time that spatiotemporal-resolved Raman spectroscopy is successfully applied to in situ measurement of electrochemical oscillations. This in situ detecting technique is expected to provide us with a powerful experimental tool to elucidate the mechanisms for other electrochemical oscillatory systems.

**Spatial-Resolved Raman Spectroscopy.** The depletion of the iodate concentration near the surface at a constant potential control of  $-1.3 \text{ V}$  was shown in Figure 2, where the spatial-resolved Raman spectra (Figure 2A) were obtained by changing the distance between the laser focus and the working electrode surface. A concentration profile of iodate (Figure 2B) in the

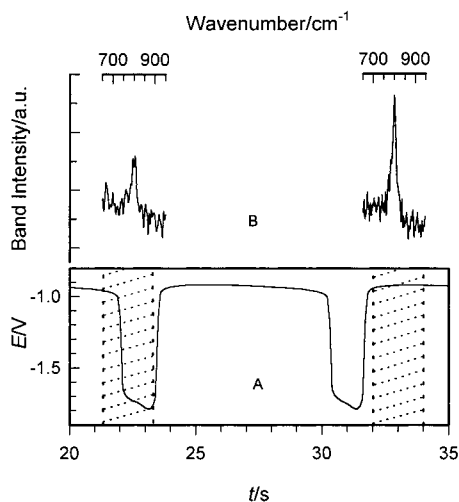


**Figure 3.** In situ Raman spectra during the potential oscillation at  $-2.5$  mA, which were taken in 2 s (shaded area) with a distance of  $40$   $\mu\text{m}$  from the surface with a same solution as used in Figure 1.

diffusion layer was obtained by the spatial-resolved Raman spectra. It is clearly seen that the reduction of iodate is diffusion-controlled in the potential range of the limiting current plateau.

**Time-Resolved Raman Spectroscopy.** Time-resolved Raman spectra were taken during the potential oscillations at a fixed distance of  $40$   $\mu\text{m}$  from the electrode surface. With the depletion of the iodate concentration, the potential shifts to the negative side of the plateau (left shaded area of Figure 3A), and the band intensity of the measured spectrum (on the left of Figure 3B) is lower. The band intensity of the spectrum increases (on the right of Figure 3B) while the iodate concentration is restored by the convection feedback through hydrogen evolution at the lower potential side of the plateau, and the potential then returns to the positive side of the plateau (right shaded area of Figure 3A). These experimental results provide direct evidence for the diffusion-limited depletion and the convection-enhanced replenishment processes of the reactant surface concentration, and they also indicate that the thickness of the diffusion layer varies with the alternation of the depletion and the replenishment. So the assumptions of a constant diffusion layer thickness and a linear concentration profile in ref 6 seem to be oversimplified approximations, whereas the assumption that the iodate in the double layer is provided only by the diffusion mass transfer (eq 5a of ref 6) is simply wrong. How can the iodate surface concentration be restored during the oscillations by only diffusion mass transfer, while the applied current is beyond the limiting current? It is common knowledge that the surface concentration is always at zero under limiting diffusion without the convection feedback.

**Further Evidence for the Convection Feedback.** Since potential oscillations for the reduction of  $\text{Fe}(\text{CN})_6^{3-}$  (Figure 4a) and  $\text{IO}_3^-$  (Figure 1B) in alkaline solution accompanying periodic hydrogen evolution belong to same category of oscillators as claimed by the authors of both mechanisms,<sup>2,3,6</sup> noticing that they all appear above the limiting current, a convenient experimental method to test the effect of the convection feedback has been designed by simply replacing the hydrogen evolution reaction with another pure current carrier  $\text{IO}_3^-$  during the  $\text{Fe}(\text{CN})_6^{3-}$  reduction.<sup>10</sup> In this way, we can only remove the convection mass transfer induced by the hydrogen evolution while the NDR from the Frumkin repulsive effect is maintained.

From Figure 4b we can see that after adding  $\text{IO}_3^-$  the length of the limiting current plateau for the reduction of  $\text{Fe}(\text{CN})_6^{3-}$  is shortened with the lower potential limit at ca.  $-1$  V, where

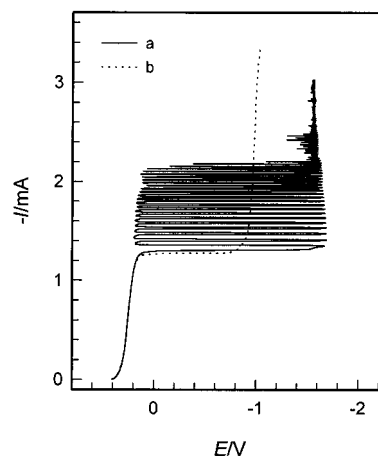


**Figure 4.** Current scan at  $0.01$  mA  $\text{s}^{-1}$  in  $1$  mol  $\text{dm}^{-3}$  NaOH solutions containing (a)  $0.6$  mol  $\text{dm}^{-3}$   $\text{Fe}(\text{CN})_6^{3-}$  and (b)  $0.15$  mol  $\text{dm}^{-3}$   $\text{IO}_3^-$  +  $0.6$  mol  $\text{dm}^{-3}$   $\text{Fe}(\text{CN})_6^{3-}$ .

the reduction current of  $\text{IO}_3^-$  replaces the hydrogen evolution current and the convection mass transfer induced by the gas evolution is eliminated. In this case, no oscillations occur for the  $\text{Fe}(\text{CN})_6^{3-}$  reduction in the same current range. This experimental result gives another direct evidence for the convection feedback step of mechanism A. It is also clearly shown in Figure 4b that purely a second current carrier  $\text{IO}_3^-$  in the second ascending branch can only conduct the extra current when the applied current is larger than the  $\text{Fe}(\text{CN})_6^{3-}$  limiting reduction current, and there is no an efficient way to restore the surface concentration of  $\text{Fe}(\text{CN})_6^{3-}$  when it depletes to zero. Because there is no convection feedback induced by the hydrogen evolution, the  $\text{Fe}(\text{CN})_6^{3-}$  surface concentration is always at zero under limiting diffusion, and that is the reason no oscillations occur with the replacement. This experimental result confirms once again the incorrectness of eq 5a of ref 6, in which only diffusion mass transfer is taken into consideration for the increase of iodate concentration in the diffusion layer. A constant stronger agitation can also stop the oscillation<sup>2,6</sup> by means of preventing the  $\text{IO}_3^-$  surface concentration from depleting. This fact implies that alternately predominant diffusion and convection mass transfer of the reactant is crucial for this category of oscillators.

Koper<sup>11</sup> once summarized that negative impedance or NDR<sup>6</sup> can result from three causes: (i) a negative  $dk_f(E)/dE$ , i.e., a heterogeneous rate constant that decrease with increasing polarization in some potential interval; (ii) a negative  $dc^0/dE$ , i.e., a Coulombic (double layer) repulsion between the electroactive species and the electrode; and (iii) a negative  $dA/dE$ , i.e., a decrease in the available surface area with increase  $E$ , for instance as the result of the adsorption on the electrode of an inhibitor. Koper only related the NDR to current oscillations.<sup>12</sup>

However, all those causes, if any can be used to explain the potential oscillation,<sup>6</sup> can at most describe the positive feedback step. The main reason the NDR is not applicable to this category of oscillators is that the NDR-based model<sup>6</sup> fails to reflect the convection negative feedback step present in the oscillation. To oscillate in two states, as we know, positive and negative feedback steps must coexist between them.

Moreover, the positive feedback mainly stems from the diffusion-limited depletion rather than from the Frumkin repulsive effect,<sup>6</sup> as we have pointed out that the descending branch in the N-shaped curve during the forward scan in Figure 1A results from the depletion of the reactant surface concentration.

In addition, the fact that the hidden negative impedance or HNDR (Figure 3 in ref 6) appears at nonzero frequency only, and the real part of the impedance at zero frequency is absolutely positive, also indicates that the potential-dependent kinetic process is a relatively rapid one and can be only shown with a faster perturbation in the frequency domain. Koper pointed out that the HNDR requires the coupling of at least two potential-dependent processes<sup>12</sup> and related the HNDR to both current and potential oscillations. Although potential-dependent causes might be responsible for the HNDR, they have nothing to do with this category of oscillators, because the reduction of the reactant is diffusion-limited and the oscillation occurs only above the limiting current. In other words, the reason for the negative impedance (mainly from the potential-dependent processes) and for the oscillation (mainly involving mass transfer) is not the same at least for this category of oscillators, as we have already discussed from the viewpoint of nonlinear feedbacks. Our purpose here is to elucidate the oscillatory mechanism rather than the hidden negative impedance, since they do not show a direct connection for the system studied as we have evidenced experimentally. To further clear up the misunderstanding, we would also like to remind the reader that it is certainly not the first time that the negative impedance cannot give an explanation for the electrochemical oscillation, as Koper himself admitted several years ago,<sup>13</sup> which has been further confirmed recently by Nakato et al.<sup>14</sup> The fact is that NDR or HNDR can explain some but not every electrochemical oscillation, and we have clearly shown why the NDR-based mechanism is not applicable to this category of oscillators that mainly involves mass transfer.

## Conclusions

A pair of overlapping positive and negative feedbacks from the diffusion-controlled depletion and from the convection-induced replenishment between the bistable states, i.e., with and without hydrogen evolution, account for the galvanostatic potential oscillation in the reduction of  $\text{IO}_3^-$  accompanying periodic hydrogen evolution. The mechanism has been further confirmed by in situ spatiotemporal-resolved Raman spectroscopy and electrochemical measurements, and it is the origin for the same category of electrochemical oscillators from the coupling of electrochemical reaction mainly with mass transfer

as in the reduction of ferricyanide,<sup>3</sup> peroxodisulfate,<sup>4</sup> and hydrogen peroxide<sup>5</sup> involving hydrogen evolution and in the oxidation of ferrocyanide<sup>15</sup> involving oxygen evolution in alkaline solution.

The descending branch in the N-shaped  $I/E$  curve obtained experimentally is due to the diffusion-limited depletion with a faster potential sweep (e.g., 100 mV/s), rather than from the Frumkin repulsive effect. A limiting current plateau occurs with a slow potential scan (e.g., 2 mV/s). The reason for the hidden NDR (mainly from potential-dependent processes) and for the oscillations (mainly involving mass transfer) has been proved to be not the same for this category of oscillators. The NDR-based mechanism that neglects the important process of convection negative feedback does not correctly account for this category of oscillators and is thus being rejected.

**Acknowledgment.** Financial support by National Natural Science Foundation of China (20073012, 29833060, 29903009) and the Visiting Scholar Foundation in State Key Labs of Ministry of Education of China is gratefully acknowledged.

## References and Notes

- (1) Radkov, E. V.; Ljutov, L. G. *J. Electroanal. Chem.* **1988**, *241*, 349.
- (2) Li, Z. L.; Cai, J. L.; Zhou, S. M. *J. Chem. Soc., Faraday Trans.* **1997**, *93*, 3519.
- (3) Li, Z. L.; Cai, J. L.; Zhou, S. M. *J. Electroanal. Chem.* **1997**, *432*, 111.
- (4) Li, Z. L.; Wu, T. H.; Chen, K. *Chin. J. Chem. Phys.* **1999**, *12*, 251.
- (5) Li, Z. L.; Zeng, Y.; Xie, Q. J.; Yao, S. Z. *J. Electrochem. Soc.* **1998**, *145*, 3857.
- (6) Strasser, P.; Lübke, M.; Eickes C.; Eiswirth, M. *J. Electroanal. Chem.* **1999**, *462*, 19.
- (7) Tian, Z. Q.; Ren, B.; Mao, B. W. *J. Phys. Chem. B*, **1997**, *101*, 1338.
- (8) Ren, B. Ph.D. Thesis, Xiamen University, Xiamen, 1998.
- (9) Li, Z. L.; Yu, Y.; Liao, H.; Yao, S. Z. *Chem. Lett.* **2000**, (4), 330.
- (10) Li, Z. L.; Yuan, Q. H.; Ren, B.; Xiao, X. M.; Zeng, Y.; Tian, Z. Q. *Electrochem. Commun.* **2001**, *3*, 654.
- (11) Koper, M. T. M. *Electrochim. Acta*, **1992**, *37*, 1771.
- (12) Koper, M. T. M. *J. Electroanal. Chem.* **1996**, *409*, 175.
- (13) Van Venrooij, T. G. J.; Koper, M. T. M. *Electrochim. Acta*, **1995**, *40*, 1689.
- (14) Mukoyama, Y.; Nakanishi, S.; Konishi, H.; Ikeshima, Y.; Nakato, Y. *J. Phys. Chem. B*, **2001**, *105*, 10905.
- (15) Li, Z. L.; Cai, J. L.; Zhou, S. M. *J. Electroanal. Chem.* **1997**, *436*, 195.